ACS ORGANIC & INORGANIC Au
AN OPEN ACCESS JOURNAL OF THE AMERICAN CHEMICAL SOCIETY

pubs.acs.org/orginorgau

Article

Selective Oxidation of Methane to Methanol via In Situ H_2O_2 Synthesis

Fenglou Ni, Thomas Richards, Louise R. Smith, David J. Morgan, Thomas E. Davies, Richard J. Lewis,* and Graham J. Hutchings*

Cite This: *ACS Org. Inorg. Au* 2023, 3, 177−183

Read Online

ACCESS | Metrics & More | Article Recommendations | Supporting Information

ABSTRACT: The selective oxidation of methane to methanol, using H_2O_2 generated in situ from the elements, has been investigated using a series of ZSM-5-supported AuPd catalysts of varying elemental composition, prepared via a deposition precipitation protocol. The alloying of Pd with Au was found to offer significantly improved efficacy, compared to that observed over monometallic analogues. Complementary studies into catalytic performance toward the direct synthesis and subsequent degradation of H_2O_2, under idealized conditions, indicate that methane oxidation efficacy is not directly related to H_2O_2 production rates, and it is considered that the known ability of Au to promote the release of reactive oxygen species is the underlying cause for the improved performance of the bimetallic catalysts.

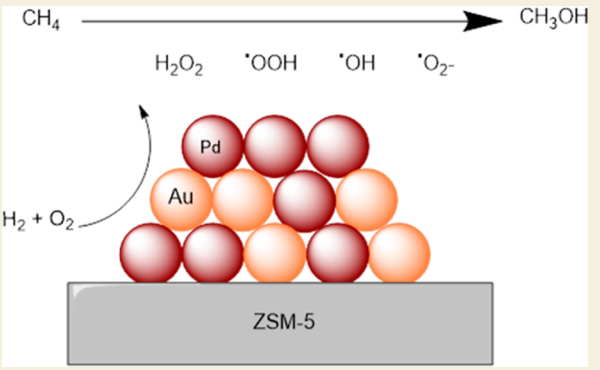

KEYWORDS: *methane oxidation, hydrogen peroxide, green chemistry, gold, palladium*

INTRODUCTION

Natural gas has long been considered a bridging feedstock to enable a transition away from a petroleum-dependent global economy. However, the selective valorization of its principal components (methane and ethane), under reaction conditions that are environmentally benign, is yet to be realized. In particular, the oxidation of methane to methanol, a valuable platform chemical with global demand estimated at 22 billion gallons/annum,[1] represents a long-standing challenge of catalysis, which is perhaps more pertinent now more than ever given aspirations to reach net zero carbon emissions. Indeed, with 142 BCM of natural gas flared in 2020 (equivalent to approximately 4% of global production[2]), the selective oxidation of methane is set to continue to remain a major area of research interest for the foreseeable future.

Currently, industrial methanol production is dominated by an energy-intensive two-step process, where methane is first converted to syngas (CO and H_2). In recent years the valorisation of methane via the in situ production of H_2O_2 has been an area of considerable academic interest,[3−6] utilizing lower temperatures (<80 °C) to alternative thermal catalytic routes.[7−10] In particular, the in situ approach would offer improved economic viability compared to the use of the preformed oxidant, with the cost of commercial H_2O_2 typically being in excess of methanol itself. Additionally, the in situ route has been widely reported to offer improved methanol selectivity compared to that observed when using ex situ H_2O_2,[11] although in general methanol formation rates are often considerably lower when H_2O_2 is generated in situ from the elements.[5]

The use of the aluminosilicate ZSM-5 within methane oxidation has received considerable attention, while such studies have typically focused on biomimetic oxidation, utilizing Fe and/or Cu species incorporated into the zeolite framework in conjunction with preformed H_2O_2.[12−17] Additionally, there has been growing attention placed on the use of ZSM-5 as a support for active metal species for both the direct synthesis of H_2O_2[18−22] and in situ oxidation of methane to methanol.[23] Recently Jin et al. reported that enhanced rates of methane oxidation via in situ H_2O_2 synthesis can be achieved through the introduction of a hydrophobic organo-silane layer onto the external surface of a AuPd@ZSM-5 catalyst, with the improved reactivity attributed to the increased localized concentrations of reagents (H_2 and O_2), and the confinement of the subsequently synthesized H_2O_2 and CH_4 in close proximity to active sites.[24]

With these earlier studies in mind, we now investigate the activity of AuPd nanoalloys immobilized onto a commercially available ZSM-5 support for the valorization of methane via the

Received: January 5, 2023
Revised: April 13, 2023
Accepted: April 13, 2023
Published: April 20, 2023

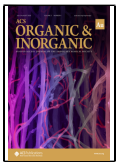

Table 1. Catalytic Activity of 0.5%AuPd/ZSM-5 Catalysts toward the Direct Synthesis and Subsequent Degradation of H_2O_2 as a Function of the Au/Pd Ratio[a]

catalyst	productivity ($mol_{H_2O_2}$ kg_{cat}^{-1} h^{-1})	H_2O_2 conc. (ppm)	degradation ($mol_{H_2O_2}$ kg_{cat}^{-1} h^{-1})
ZSM-5	0	0	12
0.5%Au/ZSM-5	2	100	20
0.475%Au-0.025%Pd/ZSM-5	3	110	35
0.375%Au-0.125%Pd/ZSM-5	7	460	58
0.25%Au-0.25%Pd/ZSM-5	9	720	68
0.125%Au-0.375%Pd/ZSM-5	10	732	104
0.025%Au-0.475%Pd/ZSM-5	12	761	112
0.5%Pd/ZSM-5	12	786	116

[a]H_2O_2 direct synthesis reaction conditions: catalyst (0.01 g), H_2O (2.9 g), MeOH (5.6 g), 5% H_2/CO_2 (420 psi), 25% O_2/CO_2 (160 psi), 0.5 h, 2 °C, 1200 rpm. H_2O_2 degradation reaction conditions: catalyst (0.01 g), H_2O_2 (50 wt %, 0.68 g), H_2O (2.22 g), MeOH (5.6 g), 5% H_2/CO_2 (420 psi), 0.5 h, 2 °C, 1200 rpm.

Table 2. Effect of Au/Pd Ratio on the Activity of 0.5%AuPd/ZSM-5 Catalysts toward the Oxidation of Methane to Methanol via In Situ H_2O_2 Production[a]

	products (μmol)					
catalyst	CH_3OH	CH_3OOH	HCOOH	CO_2	productivity ($\mu mol_{oxygenates}$ g_{cat}^{-1})	TOF (h^{-1})
ZSM-5	0	0	0		0	0
0.5%Au/ZSM-5	0	0	0		0	0
0.475%Au-0.025%Pd/ZSM-5	0.143	0	0		5.3	0.39
0.375%Au-0.125%Pd/ZSM-5	0.188	0	0		7.0	0.44
0.25%Au-0.25%Pd/ZSM-5	0.290	0	0		10.7	0.57
0.125%Au-0.375%Pd/ZSM-5	0.205	0	0		7.6	0.35
0.025%Au-0.475%Pd/ZSM-5	0.056	0	0		2.1	0.09
0.5%Pd/ZSM-5	0	0	0		0	0

[a]Methane oxidation reaction conditions: catalyst (0.028 g), H_2O (10.0 g), 435 psi total pressure (0.8% H_2/1.6% O_2/76.7% CH_4/20.8% N_2), 0.5 h, 50 °C, 1500 rpm. Note 1: For all catalyst formulations, CO_2 production was found to be within experimental error of the blank reaction. Note 2: Turnover frequency (TOF) calculated using the total moles of product and based on theoretical metal loading.

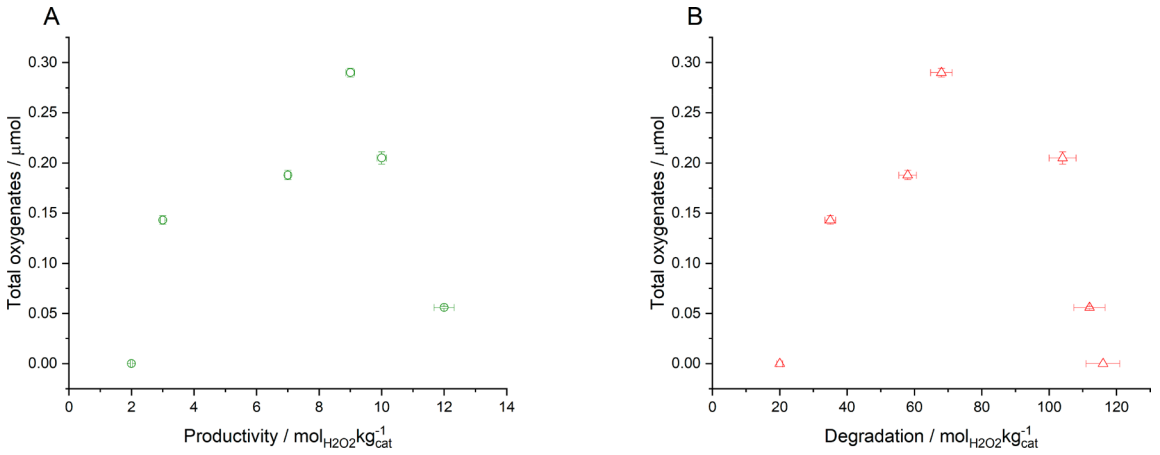

Figure 1. Correlation between catalytic activity toward the in situ selective oxidation of methane and (A) the direct synthesis and (B) subsequent degradation of H_2O_2. H_2O_2 direct synthesis reaction conditions: catalyst (0.01 g), H_2O (2.9 g), MeOH (5.6 g), 5% H_2/CO_2 (420 psi), 25% O_2/CO_2 (160 psi), 0.5 h, 2 °C, 1200 rpm. H_2O_2 degradation reaction conditions: catalyst (0.01 g), H_2O_2 (50 wt %, 0.68 g), H_2O (2.22 g), MeOH (5.6 g), 5% H_2/CO_2 (420 psi), 0.5 h, 2 °C, 1200 rpm. Methane oxidation reaction conditions: catalyst (0.027 g), H_2O (10.0 g), 435 psi total pressure (0.8% H_2/1.6% O_2/76.7% CH_4/20.8% N_2), 0.5 h, 50 °C, 1500 rpm.

in situ production of H_2O_2, with an aim to gain further insight into the efficacy of such catalytic systems and further develop an in situ approach to alkane upgrading.

RESULTS AND DISCUSSION

Our initial studies via X-ray diffraction (XRD) (Figure S1, supplementary note 1) and Fourier transform infrared (FTIR) spectroscopy (Figure S2, supplementary note 2) established that the synthesis and thermal treatment of the AuPd/ZSM-5 catalysts resulted in no significant detrimental effects on zeolitic structure, as evidenced by comparison to the as-supplied ZSM-5 support. Notably, our XRD analysis revealed no clear reflections associated with immobilized metals, which may be expected given the low total metal loading of these materials. The textural properties of key synthesized catalysts are summarized in Table S1. In keeping with previous

https://doi.org/10.1021/acsorginorgau.3c00001
ACS Org. Inorg. Au 2023, 3, 177−183

investigations[25] the immobilization of active metals resulted in a general decrease in both total surface area and micropore volume in comparison to the bare zeolitic material, with this attributed to the deposition of metal species within the zeolitic pore structure.

Using reaction conditions that have previously been optimized to promote H_2O_2 stability,[26] our initial studies established the effect of Au/Pd ratio (actual metal loading, as determined by digestion of as-prepared catalysts and MP-AES analysis reported in Table S2) on catalytic reactivity toward the direct synthesis and subsequent degradation of H_2O_2 (Table 1, an investigation into catalyst reusability is presented in Table S3). In keeping with recent works into AuPd nanoalloys supported on zeolite[25] and silica supports,[27] we observed a direct correlation between catalytic activity toward both the direct synthesis and subsequent degradation of H_2O_2 and Pd content, with the 0.5%Pd/ZSM-5 catalyst offering rates of H_2O_2 production (12 $mol_{H_2O_2}$ kg_{cat}^{-1} h^{-1}) somewhat higher than 0.25%Au-0.25%Pd/ZSM-5 analogue (9 $mol_{H_2O_2}$ kg_{cat}^{-1} h^{-1}). However, the bimetallic catalyst was found to be far more selective, with H_2O_2 degradation rates (68 $mol_{H_2O_2}$ kg_{cat}^{-1} h^{-1}) significantly lower than those of the Pd-only catalyst (112 $mol_{H_2O_2}$ kg_{cat}^{-1} h^{-1}).

Evaluation of the catalytic series toward the oxidation of methane, via in situ H_2O_2 production, is reported in Table 2, with a comparison of catalytic performance toward oxygenate formation during the in situ oxidation of methane and activity toward H_2O_2 synthesis and degradation reported in Figure 1A,B. A wider comparison of the catalytic performance of the materials investigated in this work to those previously investigated in the literature using in situ-generated H_2O_2 is reported in Table S.4. Catalytic activity toward methane oxidation was not found to follow the same trend as that observed for H_2O_2 direct synthesis (Table 1), with the bimetallic formulations achieving higher rates of methane oxidation than that observed over the monometallic Pd catalyst, despite the greater activity of this formulation toward H_2O_2 synthesis. Indeed, it is notable that the Pd-only catalyst displayed no activity toward the in situ oxidation of methane. Such observations may indicate that the observed reactivity trends for in situ methane oxidation may not be wholly related to H_2O_2 production. When considered alongside earlier works which have reported the ability of Au to promote the desorption of reactive oxygen species (•OOH, •OH, and $•O_2^-$),[28,29] in addition to H_2O_2,[30] from catalytic surfaces. It is possible to suggest that in addition to H_2O_2, there is a significant contribution to the observed catalysis from intermediate species generated during the formation of H_2O_2. Such observations would align well with earlier works that have identified the crucial role of •OH formation, from H_2O_2, and the resulting activation of methane via H-abstraction.[31] It should be noted that regardless of catalyst formulation, total selectivity toward methanol was observed, which can be related to the relatively low reactivity of the materials studied.

The selectivity of Pd-based catalysts toward H_2O_2 has been widely reported to be related to particle size, with the high proportion of defect sites present in smaller particles considered to be responsible for H_2O_2 degradation.[32,33] Similar activity trends have also been reported for the selective oxidation of methane to methanol when supported AuPd nanoalloys were utilized in conjunction with preformed H_2O_2.[3] Determination of the mean nanoparticle size of key catalysts via transmission electron microscopy (TEM) (Table 3, with corresponding electron micrographs reported in Figure S3) reveals a minimal variation of this metric across the catalytic series. As such it is possible to conclude that catalytic trends are not dependent on particle size effects.

Table 3. Mean Particle Size of 0.5%AuPd/ZSM-5 Catalysts as Determined via TEM[a]

catalyst	mean particle size (nm) (standard deviation)
0.5%Au/ZSM-5	6.5 (2.2)
0.25%Au-0.25%Pd/ZSM-5	4.1 (1.3)
0.5%Pd/ZSM-5	4.1 (1.1)

[a]Note: All catalysts were exposed to a reductive heat treatment (3 h, 400 °C, 10 °C min^{-1}, 5%H_2/Ar).

X-ray photoelectron spectroscopic (XPS) evaluation of the as-prepared AuPd/ZSM-5 catalysts and analogous spent materials is shown in Table 4, with representative spectra reported in Figure S4. Evident from our analysis is the marked difference in the Au/Pd ratio between the fresh and used catalysts, although in all cases both Au and more interestingly Pd are found to exist in the metallic state, with the enhanced activity of Pd^0 species, compared to Pd^{2+} analogues well reported for H_2O_2 direct synthesis.[34] Subtle changes in the Si/Al ratio should also be noted and are indicative of an increase in the surface Al content. In all instances, after use in the methane oxidation reaction, the amount of Au was observed to decrease relative to that of Pd, with such observations possibly indicative of the agglomeration or leaching of metal species.

Table 4. XPS-Derived Au/Pd and Si/Al Ratios for Fresh and Used 0.5%AuPd/ZSM-5 Catalysts[a]

	Au/Pd		Si/Al	
catalyst	fresh	used	fresh	used
0.5%Au/ZSM-5	n/a	n/a	11.4	12.4
0.475%Au-0.025%Pd/ZSM-5	13.0	n/d	11.4	12.4
0.375%Au-0.125%Pd/ZSM-5	0.78	0.25	12.1	12.5
0.25%Au-0.25%Pd/ZSM-5	0.50	0.07	12.1	12.6
0.125%Au-0.375%Pd/ZSM-5	0.17	0.36	11.9	12.3
0.025%Au-0.475%Pd/ZSM-5	n/d	n/d	11.2	11.8
0.5%Pd/ZSM-5	n/a	n/a	11.7	12.4

[a]Note: n/a = not applicable, n/d = unable to determine due to low concentration of metal.

Given the potential for structural modification or metal leaching indicated by our analysis by XPS, we subsequently conducted a detailed analysis of the as-prepared 0.25%Au-0.25%Pd/ZSM-5 catalyst after use in the in situ methane oxidation reaction (Figure 2A,B). Such analysis identified a broad particle size distribution with the larger particles (>5 nm) observed to be Au-rich AuPd alloys, primarily of a Au-core, Pd-shell morphology. By comparison, the smaller nanoparticles (<5 nm) were found to consist of Pd only. Notably, no clear variation in particle composition or size was observed between the fresh and used samples. We subsequently investigated the stability of the catalytic series through MP-AES analysis of post-reaction solutions (Table 5). These studies confirmed the loss of both Au and Pd upon use, which may explain the elemental variation observed via XPS analysis; however, the extent of such leaching was relatively

https://doi.org/10.1021/acsorginorgau.3c00001
ACS Org. Inorg. Au 2023, 3, 177−183

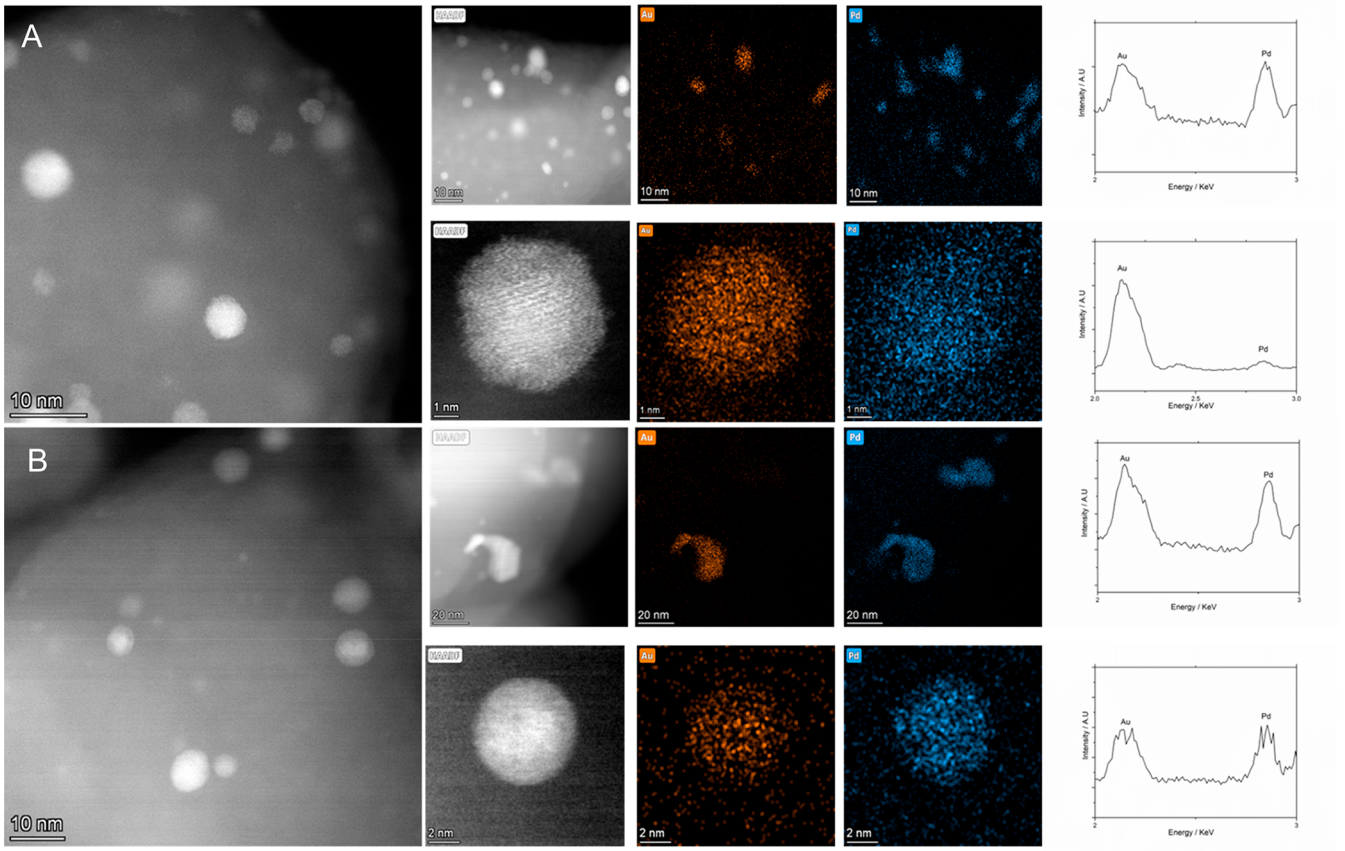

Figure 2. High-angle annular dark-field scanning transmission electron microscopy analysis of the (A) as-prepared 0.25%Au-0.25%Pd/ZSM-5 catalyst and (B) after use in the in situ oxidation of the methane reaction. Corresponding EDX mapping and spectra are also reported [Au (Mα) and Pd (Lα)] centered at 2.12 and 2.84 keV, respectively. The larger particles are shown to be Au-rich AuPd alloys and the smaller particles primarily Pd.

Table 5. Metal Leaching during the Selective Oxidation of Methane via In Situ H_2O_2 Synthesis, as Determined from MP-AES Analysis of Postreaction Solutions[a]

	metal leached (%)	
catalyst	Au	Pd
0.5%Au/ZSM-5	1.4	
0.475%Au-0.025%Pd/ZSM-5	0.9	2.1
0.375%Au-0.125%Pd/ZSM-5	0.6	1.1
0.25%Au-0.25%Pd/ZSM-5	0.4	0.6
0.125%Au-0.375%Pd/ZSM-5	3.6	4.2
0.025%Au-0.475%Pd/ZSM-5	1.8	1.8
0.5%Pd/ZSM-5		1.5

[a]Methane oxidation reaction conditions: catalyst (0.027 g), H_2O (10.0 g), 435 psi total pressure (0.8% H_2/1.6% O_2/76.7% CH_4/20.8% N_2), 0.5 h, 50 °C, 1500 rpm.

low. Regardless, it is clear that further efforts to promote catalyst stability are still required, in particular given the known activity of homogeneous metal species to catalyze both the direct synthesis of H_2O_2[35] and the oxidation of methane.[36]

CONCLUSION

The selective valorization of methane to methanol via the in situ synthesis of H_2O_2 represents an attractive, low-temperature alternative to current industrial routes to this platform chemical and would avoid the significant costs associated with the use of commercial H_2O_2. Within this work, using low-loaded AuPd nanoalloys immobilized onto a ZSM-5 support, we demonstrate the key role of Au and Pd content on catalytic performance, with materials which consist of a Au/Pd ratio approaching 1:1 shown to offer enhanced reactivity. This is despite the improved performance of the Pd-only analogue toward H_2O_2 production, under conditions idealized for H_2O_2 stability. Such trends may indicate the key role of alternative reactive oxygen species for methane oxidation and would align well with recent findings. While catalyst stability is of concern, we consider that these materials represent a promising basis for further exploration for the selective oxidation of a range of feedstocks, in particular given their high selectivity toward methanol.

EXPERIMENTAL SECTION

Catalyst Preparation

Prior to co-deposition of metal salts, NH_4-ZSM-5 (Zeolyst) was calcined in flowing air (450 °C, 6 h, 3 °C min^{-1}) according to our previous work.[37] Mono- and bimetallic 0.5%Au−Pd/ZSM-5 catalysts have been prepared (on a weight metal basis) by the co-deposition of metal salts, based on a methodology previously reported in the literature.[7] The procedure to produce the 0.25%Au−0.25%Pd/ZSM-5 catalyst (1 g) is outlined below.

$PdCl_2$ (0.42 mL, [Pd] = 6 mg mL^{-1}, Sigma-Aldrich) and $HAuCl_4 \cdot 3H_2O$ solution (0.21 mL, [Au] = 12.25 mg mL^{-1}, Strem Chemicals) were charged into deionized water (67 mL), under stirring (600 rpm), followed by the addition of the ZSM-5 support (0.995 g). Subsequently, NH_4OH (2.5 wt %) was added dropwise over 30 min, finally reaching a pH of 6. The temperature of the resulting slurry

https://doi.org/10.1021/acsorginorgau.3c00001
ACS Org. Inorg. Au 2023, 3, 177−183

was increased to 60 °C and aged for 2 h with stirring (600 rpm), followed by separation of the solid catalyst via filtration and subsequent washing with deionized water (800 mL). The recovered catalyst was then ground and dried under vacuum (60 °C, 16 h) prior to heat treatment (5%H_2/Ar, 400 °C, 3 h, 10 °C min^{-1}).

Catalyst Testing

Note 1: For both H_2O_2 direct synthesis and degradation experiments, the reactor temperature was controlled using a HAAKE K50 bath/circulator using an appropriate coolant. Reactor temperature was maintained at 2 ± 0.2 °C throughout the course of the H_2O_2 synthesis and degradation reaction.

Note 2: The conditions used within this work for H_2O_2 synthesis and degradation have previously been investigated, with the use of subambient reaction temperatures, CO_2 reactant gas diluent and a methanol co-solvent identified as key to maintaining high catalytic efficacy toward H_2O_2 production.[26] In particular the CO_2 gaseous diluent, has been found to act as an in situ promoter of H_2O_2 stability through dissolution in the reaction solution and the formation of carbonic acid. We have previously reported that the use of the CO_2 diluent has a comparable promotive effect to that observed when acidifying the reaction solution to a pH of 4 using HNO_3.[38]

Note 3: In all cases, reactions were run multiple times, over multiple batches of catalyst, with the data being presented as an average of these experiments.

Direct Synthesis of H_2O_2

Hydrogen peroxide synthesis was evaluated by using a Parr Instruments stainless steel autoclave with a nominal volume of 100 mL and a maximum working pressure of 2000 psi. To test each catalyst for H_2O_2 synthesis, the autoclave was charged with catalyst (0.01 g) and solvent (5.6 g methanol and 2.9 g H_2O, Fischer Scientific, HPLC standard). The charged autoclave was then purged three times with 5% H_2/CO_2 (100 psi) before filling with 5% H_2/CO_2 to a pressure of 420 psi, followed by the addition of 25% O_2/CO_2 (160 psi). The reaction was conducted at a temperature of 2 °C, for 0.5 h with stirring (1200 rpm). Reactant gases were not continuously supplied. H_2O_2 productivity was determined by titrating aliquots of the final solution after reaction with acidified $Ce(SO_4)_2$ (0.0085 M) in the presence of a ferroin indicator. Catalyst productivities are reported as $mol_{H_2O_2}\ kg_{cat}^{-1}\ h^{-1}$.

Catalytic conversion of H_2 and selectivity toward H_2O_2 were determined using a Varian 3800 GC fitted with TCD and equipped with a Porapak Q column.

H_2O_2 selectivity (eq 1) is defined as follows:

$$H_2O_2\ \text{selectivity}\ (\%) = \frac{H_2O_2\ \text{detected (mmol)}}{H_2\ \text{consumed (mmol)}} \times 100 \quad (1)$$

Degradation of H_2O_2

Catalytic activity toward H_2O_2 degradation was determined in a similar manner to the direct synthesis activity of a catalyst. The autoclave was charged with methanol (5.6 g, Fischer Scientific, HPLC standard), H_2O_2 (50 wt % 0.68 g, Merck), H_2O (2.22 g, Fischer Scientific HPLC standard), and catalyst (0.01 g), with the solvent composition equivalent to a 4 wt % H_2O_2 solution. From the solution, two aliquots of 0.05 g were removed and titrated with acidified $Ce(SO_4)_2$ solution using ferroin as an indicator to determine an accurate concentration of H_2O_2 at the start of the reaction. The autoclave was pressurized with 5% H_2/CO_2 (420 psi). The reaction was conducted at a temperature of 2 °C, for 0.5 h with stirring (1200 rpm). After the reaction was complete, the catalyst was removed from the reaction mixture and two aliquots of 0.05 g were titrated against the acidified $Ce(SO_4)_2$ solution using ferroin as an indicator. The degradation activity is reported as $mol_{H_2O_2}\ kg_{cat}^{-1}\ h^{-1}$.

Catalyst Reusability in the Direct Synthesis and Degradation of H_2O_2

In order to determine catalyst reusability, a similar procedure to that outlined above for the direct synthesis of H_2O_2 is followed utilizing 0.05 g of catalyst. Following the initial test, the catalyst was recovered by filtration and dried (30 °C, 16 h, under vacuum); from the recovered catalyst sample, 0.01 g was used to conduct a standard H_2O_2 synthesis or degradation test.

Methane Oxidation Using In Situ Synthesized H_2O_2

The oxidation of methane was carried out using a Parr stainless steel autoclave with a nominal volume of a 50 mL reactor and a maximum working pressure of 2000 psi. To evaluate catalytic activity, the autoclave was charged with catalyst (0.027 g) and solvent (10 g H_2O, Fischer Scientific, HPLC grade). Subsequently, the reactor was purged with methane (100 psi) and charged with pure H_2, N_2, O_2 and CH_4 such that the total pressure equaled 435 psi. The gas phase composition was 0.8% H_2/ 1.6% O_2/ 76.7% CH_4/ 20.8% N_2 to ensure the mixture was outside of the explosive limits. The autoclave was then heated to the desired reaction temperature (50 °C); once at the set temperature, the reaction solution was stirred at 1500 rpm for 0.5 h. After the reaction was complete, the stirring was stopped and the temperature was reduced to 10 °C using ice water in order to minimize the loss of volatile products. Gaseous samples were analyzed via gas chromatography (Varian-GC, equipped with a CPSIL5CB column (50 m, 0.33 mm internal diameter) fitted with a methanizer and flame ionization detector). The reaction mixture was filtered to remove the catalyst and analyzed by ^{1}H NMR, using a Bruker 500 MHz Ultrashield NMR spectrometer. All ^{1}H NMR samples were analyzed against a calibrated insert containing tetramethylsilane in deuterated chloroform (99.9% D). The remaining H_2O_2 was determined by titration with acidified $Ce(SO_4)_2$.

Characterization

Investigation of the bulk structure of the materials was carried out using powder XRD on a (θ–θ) PANalyticalX'pert Pro powder diffractometer using a Cu Kα radiation source operating at 40 keV and 40 mA. Standard analysis was performed using a 40 min scan between 2θ values of 10 and 80° with the samples supported on an amorphous silicon wafer. Diffraction patterns of phases were identified using the ICDD database.

XPS measurements were performed on a Thermo Scientific K-Alpha$^+$ spectrometer using a monochromatic AlKα radiation source operating at 72 W (6 mA × 12 kV) which defines an analysis are of approximately 400 × 600 μm. An analyzer pass energy of 150 eV was used for survey scans and 50 eV for elemental regions, all samples were recorded using a dual ion-electron charge compensation operating with an argon background pressure of ~10^{-7} mbar. Samples were mounted by pressing on to silicone-free double-sided adhesive tape. Reported binding energies were referenced to a Si(2p) binding energy of 102.6 eV common for aluminosilicate materials, this was chosen as a more stable reference due to the low carbon concentrations on some of the materials leading to a greater deal of uncertainty in the C(1s) peak position. Spectra were quantified using CasaXPS[39] using a Shirley-type background and an electron escape depth dependence based on the TPP-2 M equation and Scofield sensitivity factors to obtain surface compositions (atom%) of the different samples.

FTIR spectroscopy was carried out with a Bruker Tensor 27 spectrometer fitted with a HgCdTe (MCT) detector and operated with OPUS software.

N_2 isotherms were collected on a Micromeritics 3Flex. Samples (~0.1 g) were degassed (250 °C, 6 h) prior to analysis. Analyses were carried out at 77 K with P0 measured continuously. Free space was measured post-analysis with He. Pore size analysis was carried out using Micromeritics 3Flex software, N_2–cylindrical pores–oxide surface DFT model.

Total metal loading and metal leaching from the supported catalysts were quantified using microwave plasma atomic emission spectroscopy (MP-AES). Fresh catalysts were digested (25 mg of catalyst, 2.5 mL of aqua regia, 24 h) prior to analysis using an Agilent 4100 MP-AES, while post-reaction solutions were also analyzed after filtration of the solid material. Metal concentrations were determined by the response at two characteristic emission wavelengths for Au (242.8 and 267.6 nm) and Pd (340.5 and 363.5 nm), and the

https://doi.org/10.1021/acsorginorgau.3c00001
ACS Org. Inorg. Au 2023, 3, 177–183

resultant concentrations were averaged. The concentration responses of Au and Pd were calibrated using commercial reference standards (Agilent); in all cases, $r^2 > 0.999$.

TEM was performed on a JEOL JEM-2100 operating at 200 kV. Samples were prepared by dispersion in ethanol via sonication and deposited on 300 mesh copper grids coated with a holey carbon film.

Aberration-corrected scanning transmission electron microscopy was performed using a probe-corrected Thermo Fisher Scientific Spectra 200 Cold-FEG operating at 200 kV. The instrument was equipped with a HAADF detector, and the imaging was done at a probe current of 120 pA and convergence angle of 30 mrad. Samples were dry dispersed onto 300 mesh copper grids coated with a holey carbon film. Energy-dispersive X-ray (EDX) mapping was performed using a Super-X G2 detector at a dwell time of 25 μs. All images and EDX data were processed using Velox software.

■ ASSOCIATED CONTENT

Data Availability Statement

The data underlying this study are available in the published article and its Supporting Information.

Supporting Information

The Supporting Information is available free of charge at https://pubs.acs.org/doi/10.1021/acsorginorgau.3c00001.

Data relating to the characterization of AuPd/ZSM-5 catalysts via XRD, FTIR, XPS, and TEM; determination of metal loading based on the digestion of as-prepared materials and porosimetry analysis (PDF)

■ AUTHOR INFORMATION

Corresponding Authors

Richard J. Lewis − *Max Planck−Cardiff Centre on the Fundamentals of Heterogeneous Catalysis FUNCAT, Cardiff Catalysis Institute, School of Chemistry, Cardiff University, Cardiff CF10 3AT, United Kingdom;* orcid.org/0000-0001-9990-7064; Email: LewisR27@cardiff.ac.uk

Graham J. Hutchings − *Max Planck−Cardiff Centre on the Fundamentals of Heterogeneous Catalysis FUNCAT, Cardiff Catalysis Institute, School of Chemistry, Cardiff University, Cardiff CF10 3AT, United Kingdom;* orcid.org/0000-0001-8885-1560; Email: Hutch@cardiff.ac.uk

Authors

Fenglou Ni − *Max Planck−Cardiff Centre on the Fundamentals of Heterogeneous Catalysis FUNCAT, Cardiff Catalysis Institute, School of Chemistry, Cardiff University, Cardiff CF10 3AT, United Kingdom*

Thomas Richards − *Max Planck−Cardiff Centre on the Fundamentals of Heterogeneous Catalysis FUNCAT, Cardiff Catalysis Institute, School of Chemistry, Cardiff University, Cardiff CF10 3AT, United Kingdom*

Louise R. Smith − *Max Planck−Cardiff Centre on the Fundamentals of Heterogeneous Catalysis FUNCAT, Cardiff Catalysis Institute, School of Chemistry, Cardiff University, Cardiff CF10 3AT, United Kingdom*

David J. Morgan − *Max Planck−Cardiff Centre on the Fundamentals of Heterogeneous Catalysis FUNCAT, Cardiff Catalysis Institute, School of Chemistry, Cardiff University, Cardiff CF10 3AT, United Kingdom; Research Complex at Harwell (RCaH), Harwell XPS, Didcot OX11 0FA, U.K.;* orcid.org/0000-0002-6571-5731

Thomas E. Davies − *Max Planck−Cardiff Centre on the Fundamentals of Heterogeneous Catalysis FUNCAT, Cardiff Catalysis Institute, School of Chemistry, Cardiff University, Cardiff CF10 3AT, United Kingdom*

Complete contact information is available at: https://pubs.acs.org/10.1021/acsorginorgau.3c00001

Author Contributions

F.N., T.R., and R.J.L. conducted experiments and data analysis. F.N., D.J.M., and T.E.D. conducted catalyst characterization and corresponding data processing. L.S., R.J.L., and G.J.H. contributed to the design of the study and provided technical advice and result interpretation. R.J.L. wrote the manuscript and the Supporting Information, and all authors commented on and amended both documents. All authors discussed and contributed to the work. F.N. and R.J.L. contributed equally to this work. CRediT: **Fenglou Ni** formal analysis (supporting), investigation (supporting), methodology (supporting), writing-review & editing (supporting); **Thomas Richards** data curation (supporting), formal analysis (supporting), investigation (supporting), methodology (supporting), writing-review & editing (supporting).

Notes

The authors declare no competing financial interest.

■ ACKNOWLEDGMENTS

XPS data collection was performed at the EPSRC National Facility for XPS ("HarwellXPS"), operated by Cardiff University and UCL, under Contract No. PR16195. The authors would like to thank the CCI-Electron Microscopy Facility which has been partially funded by the European Regional Development Fund through the Welsh Government and The Wolfson Foundation. F.N. acknowledges the Chinese Scholarship Council for funding. T.R., L.R.S., R.J.L., and G.J.H. gratefully acknowledge Cardiff University and the Max Planck Centre for Fundamental Heterogeneous Catalysis (FUNCAT) for financial support.

■ REFERENCES

(1) Dummer, N. F.; Willock, D. J.; He, Q.; Howard, M. J.; Lewis, R. J.; Qi, G.; Taylor, S. H.; Xu, J.; Bethell, D.; Kiely, C. J.; Hutchings, G. J. Methane Oxidation to Methanol. *Chem. Rev.* **2022**, DOI: 10.1021/acs.chemrev.2c00439.

(2) World Total Energy Supply by Source; https://www.iea.org/reports/key-world-energy-statistics-2021/supply (accessed 2022-12-27).

(3) Williams, C.; Carter, J. H.; Dummer, N. F.; Chow, Y. K.; Morgan, D. J.; Yacob, S.; Serna, P.; Willock, D. J.; Meyer, R. J.; Taylor, S. H.; Hutchings, G. J. Selective Oxidation of Methane to Methanol Using Supported AuPd Catalysts Prepared by Stabilizer-Free Sol-Immobilization. *ACS Catal.* **2018**, *8* (3), 2567−2576.

(4) Ab Rahim, M. H.; Armstrong, R. D.; Hammond, C.; Dimitratos, N.; Freakley, S. J.; Forde, M. M.; Morgan, D. J.; Lalev, G.; Jenkins, R. L.; Lopez-Sanchez, J. A.; Taylor, S. H.; Hutchings, G. J. Low temperature selective oxidation of methane to methanol using titania supported gold palladium copper catalysts. *Catal. Sci. Technol.* **2016**, *6* (10), 3410−3418.

(5) Ab Rahim, M. H.; Forde, M. M.; Jenkins, R. L.; Hammond, C.; He, Q.; Dimitratos, N.; Lopez-Sanchez, J. A.; Carley, A. F.; Taylor, S. H.; Willock, D. J.; Murphy, D. M.; Kiely, C. J.; Hutchings, G. J. Oxidation of Methane to Methanol with Hydrogen Peroxide Using Supported Gold-Palladium Alloy Nanoparticles. *Angew. Chem., Int. Ed.* **2013**, *52* (4), 1280−1284.

(6) Freakley, S. J.; Agarwal, N.; McVicker, R. U.; Althahban, S.; Lewis, R. J.; Morgan, D. J.; Dimitratos, N.; Kiely, C. J.; Hutchings, G. J. Gold-palladium colloids as catalysts for hydrogen peroxide

synthesis, degradation and methane oxidation: effect of the PVP stabiliser. *Catal. Sci. Technol.* **2020**, *10* (17), 5935−5944.
(7) Qi, G.; Davies, T. E.; Nasrallah, A.; Sainna, M. A.; Howe, A. G. R.; Lewis, R. J.; Quesne, M.; Catlow, C. R. A.; Willock, D. J.; He, Q.; Bethell, D.; Howard, M. J.; Murrer, B. D.; Harrison, B.; Kiely, C. J.; Zhao, X.; Deng, F.; Xu, J.; Hutchings, G. J. Au-ZSM-5 catalyses the selective oxidation of CH_4 to CH_3OH and CH_3COOH using O_2. *Nat. Catal.* **2022**, *5* (1), 45−54.
(8) Shan, J.; Li, M.; Allard, L. F.; Lee, S.; Flytzani-Stephanopoulos, M. Mild oxidation of methane to methanol or acetic acid on supported isolated rhodium catalysts. *Nature* **2017**, *551* (7682), 605−608.
(9) Parfenov, M. V.; Starokon, E. V.; Pirutko, L. V.; Panov, G. I. Quasicatalytic and catalytic oxidation of methane to methanol by nitrous oxide over FeZSM-5 zeolite. *J. Catal.* **2014**, *318*, 14−21.
(10) Starokon, E. V.; Parfenov, M. V.; Arzumanov, S. S.; Pirutko, L. V.; Stepanov, A. G.; Panov, G. I. Oxidation of methane to methanol on the surface of FeZSM-5 zeolite. *J. Catal.* **2013**, *300*, 47−54.
(11) Freakley, S. J.; Dimitratos, N.; Willock, D. J.; Taylor, S. H.; Kiely, C. J.; Hutchings, G. J. Methane Oxidation to Methanol in Water. *Acc. Chem. Res.* **2021**, *54* (11), 2614−2623.
(12) Hammond, C.; Hermans, I.; Dimitratos, N. Biomimetic Oxidation with Fe-ZSM-5 and H_2O_2? Identification of an Active, Extra-Framework Binuclear Core and an Fe^{III}-OOH Intermediate with Resonance-Enhanced Raman Spectroscopy. *ChemCatChem.* **2015**, *7* (3), 434−440.
(13) Sun, S.; Barnes, A. J.; Gong, X.; Lewis, R. J.; Dummer, N. F.; Bere, T.; Shaw, G.; Richards, N.; Morgan, D. J.; Hutchings, G. J. Lanthanum modified Fe-ZSM-5 zeolites for selective methane oxidation with H_2O_2. *Catal. Sci. Technol.* **2021**, *11* (24), 8052−8064.
(14) Yashnik, S. A.; Boltenkov, V. V.; Babushkin, D. E.; Taran, O. P.; Parmon, V. N. Methane Oxidation by H_2O_2 over Different Cu-Species of Cu-ZSM-5 Catalysts. *Top. Catal.* **2020**, *63* (1), 203−221.
(15) Olivos-Suarez, A. I.; Szecsenyi, A.; Hensen, E. J. M.; Ruiz-Martinez, J.; Pidko, E. A.; Gascon, J. Strategies for the Direct Catalytic Valorization of Methane Using Heterogeneous Catalysis: Challenges and Opportunities. *ACS Catal.* **2016**, *6* (5), 2965−2981.
(16) Kim, M. S.; Park, K. H.; Cho, S. J.; Park, E. D. Partial oxidation of methane with hydrogen peroxide over Fe-ZSM-5 catalyst. *Catal. Today* **2021**, *376*, 113−118.
(17) Szecsenyi, A.; Li, G.; Gascon, J.; Pidko, E. A. Mechanistic Complexity of Methane Oxidation with H2O2 by Single-Site Fe/ZSM-5 Catalyst. *ACS Catal.* **2018**, *8* (9), 7961−7972.
(18) Barnes, A.; Lewis, R. J.; Morgan, D. J.; Davies, T. E.; Hutchings, G. J. Improving Catalytic Activity towards the Direct Synthesis of H_2O_2 through Cu Incorporation into AuPd Catalysts. *Catalysts* **2022**, *12* (11), 1396.
(19) Lewis, R. J.; Bara-Estaun, A.; Agarwal, N.; Freakley, S. J.; Morgan, D. J.; Hutchings, G. J. The Direct Synthesis of H_2O_2 and Selective Oxidation of Methane to Methanol Using HZSM-5 Supported AuPd Catalysts. *Catal. Lett.* **2019**, *149* (11), 3066−3075.
(20) Santos, A.; Lewis, R. J.; Morgan, D. J.; Davies, T. E.; Hampton, E.; Gaskin, P.; Hutchings, G. J. The oxidative degradation of phenol via in situ H_2O_2 synthesis using Pd supported Fe-modified ZSM-5 catalysts. *Catal. Sci. Technol.* **2022**, *12* (9), 2943−2953.
(21) Jin, Z.; Liu, Y.; Wang, L.; Wang, C.; Wu, Z.; Zhu, Q.; Wang, L.; Xiao, F.-S. Direct Synthesis of Pure Aqueous H2O2 Solution within Aluminosilicate Zeolite Crystals. *ACS Catal.* **2021**, *11* (4), 1946−1951.
(22) Samanta, C.; Choudhary, V. R. Direct synthesis of H_2O_2 from H_2 and O_2 over Pd/H-beta catalyst in an aqueous acidic medium: Influence of halide ions present in the catalyst or reaction medium on H_2O_2 formation. *Catal. Commun.* **2007**, *8*, 73.
(23) Kang, J.; Park, E. D. Selective Oxidation of Methane over Fe-Zeolites by In Situ Generated H_2O_2. *Catalysts* **2020**, *10* (3), 299.
(24) Jin, Z.; Wang, L.; Zuidema, E.; Mondal, K.; Zhang, M.; Zhang, J.; Wang, C.; Meng, X.; Yang, H.; Mesters, C.; Xiao, F. Hydrophobic zeolite modification for in situ peroxide formation in methane oxidation to methanol. *Science* **2020**, *367* (6474), 193−197.
(25) Lewis, R. J.; Ueura, K.; Fukuta, Y.; Freakley, S. J.; Kang, L.; Wang, R.; He, Q.; Edwards, J. K.; Morgan, D. J.; Yamamoto, Y.; Hutchings, G. J. The Direct Synthesis of H_2O_2 Using TS-1 Supported Catalysts. *ChemCatChem.* **2019**, *11*, 1673.
(26) Santos, A.; Lewis, R. J.; Malta, G.; Howe, A. G. R.; Morgan, D. J.; Hampton, E.; Gaskin, P.; Hutchings, G. J. Direct Synthesis of Hydrogen Peroxide over Au-Pd Supported Nanoparticles under Ambient Conditions. *Ind. Eng. Chem. Res.* **2019**, *58* (28), 12623−12631.
(27) Edwards, J. K.; Parker, S. F.; Pritchard, J.; Piccinini, M.; Freakley, S. J.; He, Q.; Carley, A. F.; Kiely, C. J.; Hutchings, G. J. Effect of acid pre-treatment on AuPd/SiO_2 catalysts for the direct synthesis of hydrogen peroxide. *Catal. Sci. Technol.* **2013**, *3* (3), 812−818.
(28) Richards, T.; Harrhy, J. H.; Lewis, R. J.; Howe, A. G. R.; Suldecki, G. M.; Folli, A.; Morgan, D. J.; Davies, T. E.; Loveridge, E. J.; Crole, D. A.; Edwards, J. K.; Gaskin, P.; Kiely, C. J.; He, Q.; Murphy, D. M.; Maillard, J.; Freakley, S. J.; Hutchings, G. J. A residue-free approach to water disinfection using catalytic in situ generation of reactive oxygen species. *Nat. Catal.* **2021**, *4* (7), 575−585.
(29) Crombie, C. M.; Lewis, R. J.; Taylor, R. L.; Morgan, D. J.; Davies, T. E.; Folli, A.; Murphy, D. M.; Edwards, J. K.; Qi, J.; Jiang, H.; Kiely, C. J.; Liu, X.; Skjøth-Rasmussen, M. S.; Hutchings, G. J. Enhanced Selective Oxidation of Benzyl Alcohol via In Situ H_2O_2 Production over Supported Pd-Based Catalysts. *ACS Catal.* **2021**, *11* (5), 2701−2714.
(30) Li, J.; Ishihara, T.; Yoshizawa, K. Theoretical Revisit of the Direct Synthesis of H_2O_2 on Pd and Au@Pd Surfaces: A Comprehensive Mechanistic Study. *J. Phys. Chem., C* **2011**, *115*, 25359.
(31) Serra-Maia, R.; Michel, F. M.; Douglas, T. A.; Kang, Y.; Stach, E. A. Mechanism and Kinetics of Methane Oxidation to Methanol Catalyzed by AuPd Nanocatalysts at Low Temperature. *ACS Catal.* **2021**, *11* (5), 2837−2845.
(32) Freakley, S. J.; He, Q.; Harrhy, J. H.; Lu, L.; Crole, D. A.; Morgan, D. J.; Ntainjua, E. N.; Edwards, J. K.; Carley, A. F.; Borisevich, A. Y.; Kiely, C. J.; Hutchings, G. J. Palladium-tin catalysts for the direct synthesis of H_2O_2 with high selectivity. *Science* **2016**, *351*, 965.
(33) Tian, P.; Ding, D.; Sun, Y.; Xuan, F.; Xu, X.; Xu, J.; Han, Y. Theoretical study of size effects on the direct synthesis of hydrogen peroxide over palladium catalysts. *J. Catal.* **2019**, *369*, 95.
(34) Burch, R.; Ellis, P. R. An investigation of alternative catalytic approaches for the direct synthesis of hydrogen peroxide from hydrogen and oxygen. *Appl. Catal., B* **2003**, *42*, 203.
(35) Dissanayake, D. P.; Lunsford, J. H. Evidence for the Role of Colloidal Palladium in the Catalytic Formation of H_2O_2 from H_2 and O_2. *J. Catal.* **2002**, *206*, 173−176.
(36) Agarwal, N.; Freakley, S. J.; McVicker, R. U.; Althahban, S. M.; Dimitratos, N.; He, Q.; Morgan, D. J.; Jenkins, R. L.; Willock, D. J.; Taylor, S. H.; et al. Aqueous Au-Pd colloids catalyze selective CH_4 oxidation to CH_3OH with O_2 under mild conditions. *Science* **2017**, *358* (6360), 223−227.
(37) Xu, J.; Armstrong, R. D.; Shaw, G.; Dummer, N. F.; Freakley, S. J.; Taylor, S. H.; Hutchings, G. J. Continuous selective oxidation of methane to methanol over Cu- and Fe-modified ZSM-5 catalysts in a flow reactor. *Catal. Today* **2016**, *270*, 93−100.
(38) Edwards, J. K.; Thomas, A.; Carley, A. F.; Herzing, A. A.; Kiely, C. J.; Hutchings, G. J. Au-Pd supported nanocrystals as catalysts for the direct synthesis of hydrogen peroxide from H_2 and O_2. *Green Chem.* **2008**, *10*, 388−394.
(39) Fairley, N.; Fernandez, V.; Richard-Plouet, M.; Guillot-Deudon, C.; Walton, J.; Smith, E.; Flahaut, D.; Greiner, M.; Biesinger, M.; Tougaard, S.; Morgan, D. J.; Baltrusaitis. Systematic and collaborative approach to problem solving using X-ray photoelectron spectroscopy. *Appl. Surf. Sci.* **2021**, *5*, 100112.

https://doi.org/10.1021/acsorginorgau.3c00001
ACS Org. Inorg. Au 2023, 3, 177−183